

Photodissociation Dynamics of Cyclohexyl Cyanide and Cyclohexyl Isocyanide at 193 nm[†]

Tae Yeon Kang, Hyun Soon Choi, Seung Keun Shin, and Hong Lae Kim*

Department of Chemistry and Basic Science Research Institute, Kangwon National University, Chuncheon 200-701, Korea

Received: February 17, 2004

Photodissociation dynamics of cyclohexyl cyanide and cyclohexyl isocyanide at 193 nm has been investigated by measuring rotationally resolved laser-induced fluorescence spectra of CN fragments in the ground electronic state. From the spectra, rotational and vibrational energy distributions as well as translational energy releases in the products were obtained. A nonstatistical energy partitioning among products, the cyclohexyl and CN radicals, was observed, but the energy partitioning was very similar for both molecules with large translational energy releases. The dissociation takes place from the excited triplet states, which are strongly repulsive along the reaction coordinate via curve crossing from the initially prepared singlet state.

Introduction

Alkyl cyanides (R–CN) are more stable than their isomers, alkyl isocyanides (R–NC) by some 20 kcal/mol, and thus kinetics and mechanism of isomerization of isocyanides to cyanides in the ground electronic state have been extensively studied.¹ However, studies of photodissociation dynamics of these molecules are rather sparse. The lowest energy-allowed electronic transition may occur in the π electron systems in the CN moiety in a simple molecular orbital picture, which is in deep UV. The excited electronic state may still be bound, but dissociation would take place resulting from couplings with some dissociative coordinates. Since the nature of the excited state and the shape of potential-energy surfaces along the reaction coordinates govern the nature of the corresponding final products state, studies of the photodissociation dynamics of a pair of these molecules by measuring the energy release in the products provide an excellent chance to understand the excited electronic potential-energy surfaces of these CN-containing molecules.

Photodissociation of CH₃CN and CH₃NC was investigated by Simons and Ashfold in the vacuum ultraviolet region using various atomic resonance lamps.² The vibration and rotational energy distributions of the CN fragments were measured from the emission spectra of CN in the B state. The measured energy partitioning was explained by statistical theories invoking energy and angular momentum conservation constraints. The excited states responsible for dissociation were identified as 3p and 3s Rydberg states that they are linear for both molecules. For CH₃NC, the measured rotational population distributions of CN had a distinct shape at 147 nm, where the absorption to the excited state has in part bent π^* character. Photodissociation of CH₃CN was also investigated near 121.6 nm (Lyman- α) by Honma and co-workers by measuring emission spectra of CN from its B state and laser-induced fluorescence (LIF) spectra of H fragments.³ Measured translation and vibrational energy distributions were again well explained by the statistical theories, from which it was concluded that the dissociation should take place in the ground electronic state after internal conversion.

At 193 nm, photodissociation of CH₃CN produced CN exclusively in the ground electronic state, where the measured rotation and vibrational energies of CN were 16 and 10% of the available energy, respectively.⁴ It was claimed that the geometry and nearest-neighbor repulsion should affect the measured rotational energy distribution. Apart from alkyl cyanides, photodissociation dynamics of ethylene cyanide^{5,6} and isomers of allyl cyanides in their first UV absorption bands were recently reported.^{7–9} In these studies, the spectra of CN fragments were measured using LIF and frequency-modulated diode laser absorption spectroscopic techniques. The measured energy partitioning and distributions were well explained for these molecules by statistical theories, from which it was concluded that the dissociation should take place in the ground electronic state after internal conversion.

Photodissociation of cyclohexyl cyanide and cyclohexyl isocyanide at 193 nm produces cyclohexyl and CN radicals. Since cyclohexyl cyanide is more stable than cyclohexyl isocyanide by approximately 20 kcal/mol, the dissociation from cyclohexyl isocyanide is more exoergic. However, if the dissociation occurs in the ground electronic state following isomerization, the available energy should be the same and the energy partitioning would be similar for both molecules. In this sense, it is very interesting to measure the energy releases from the photodissociation of both molecules, which also provides a clue to understand the detailed mechanism of dissociation. In the case of aryl cyanides, Bersohn and co-workers studied photodissociation of phenyl cyanide and phenyl isocyanide at 193 nm.¹⁰ The internal and translational energies of CN measured from the LIF spectra and time-of-flight mass spectrometry were almost the same for both molecules, and the additional energy in phenyl isocyanide was found to be distributed in the phenyl radical. It was suggested that the dissociation occurs on a localized triplet surface via curve crossing from the initially prepared state.

In this article, photodissociation of cyclohexyl cyanide and cyclohexyl isocyanide was investigated by measuring rotationally resolved LIF spectra of the CN fragments. Vibrational and rotational population distributions in CN were measured from the spectra as well as the translational energy releases from analyses of Doppler profiles in the spectra. The detailed

[†] Part of the special issue "Richard Bersohn Memorial Issue".

* To whom correspondence may be addressed. E-mail: hlkim@kangwon.ac.kr.

dissociation dynamics were studied from these experimental measurements together with some quantum chemical ab initio molecular orbital calculations.

Experiments

The experiments were performed in a flow cell with conventional pump–probe geometry. The cell was evacuated at a pressure of 10^{-3} Torr with a mechanical pump, and vapor of the liquid sample at ambient temperature was slowly flowed through the cell at a pressure of about 50 mTorr, which was controlled by needle valves. The stated purity of 99% of liquid cyclohexyl cyanide and cyclohexyl isocyanide were purchased from Aldrich and used without further purification.

The photolysis light at 193 nm was the output of an ArF excimer laser (LEXTRA 50, Lambda Physik), which was unpolarized. The photolysis light beam was shaped as a circle (~ 5 mm diameter and ~ 10 mJ/cm²) with baffles inside the arms attached to the cell. The baffles also minimized the scattered radiation into the detector. The probe light used to measure the LIF spectra of CN at 389–382 nm employing the B–X transition was the output of a dye laser (HD-500, Lumonics) pumped by the third harmonic of an Nd:YAG laser (YM-800, Lumonics). The horizontally polarized dye laser output was counterpropagated collinearly to the photolysis laser beam. The power of the probe light was kept as low as possible to avoid saturation in the spectra, which was typically about 30 μ J/pulse (~ 5 mm dia.). The LIF signal vs photolysis laser power showed a linear dependence up to 20 mJ/cm², which ensured one-photon dissociation at the typical power used.

The fluorescence signal was detected with a photomultiplier tube (1P28A, Hamamatsu) mounted perpendicularly to the laser beams through cutoff filters to reduce scattered radiation of the photolysis light. The measured signal was fed to boxcars and processed with a signal processor. The delay between the pump and probe laser was typically about 100 ns and it was controlled with a digital pulse and delay generator. The sample pressure of 50 mTorr and the 100 ns delay time should provide a collisionless condition for most molecules. The measured fluorescence spectra were corrected for variation in the pump and probe laser powers and stored in a PC.

Quantum chemical ab initio molecular orbital calculations were performed to obtain the heat of formations of some compounds and to find transition-state geometries with energies for isomerization and molecular elimination reactions for the molecules studied. The calculations were carried out with the Gaussian 98 program package using 6-31 G**/MP2 level and/or using the B3LYP/DFT level for convenience.¹¹

Results

A. Internal Energies of the CN Fragments. The LIF spectra of CN (X, ν, N) produced from photodissociation of cyclohexyl cyanide and cyclohexyl isocyanide employing the ${}^2\Sigma \leftarrow {}^2\Sigma$, B \leftarrow X electronic transition are presented in Figure 1. In the spectra, the P branch bandheads of the 0–0 and 1–1 vibrational transitions clearly appear and the assignments for the R-branch rotational transitions are given on top of the spectra.¹² The individual transitions would result from excitations of pairs of the spin doublets corresponding to $J = N \pm 1/2$ in these spectra. The rotational population distributions were obtained from integrated intensities of the peaks corrected by appropriate line strength factors that are proportional to the square of the electronic transition moment, the Franck–Condon factors, and the Hönl–London factors (Figure 2).¹³ The peaks of the distributions were observed for $\nu = 0$ at $N = 14 \pm 2$ and

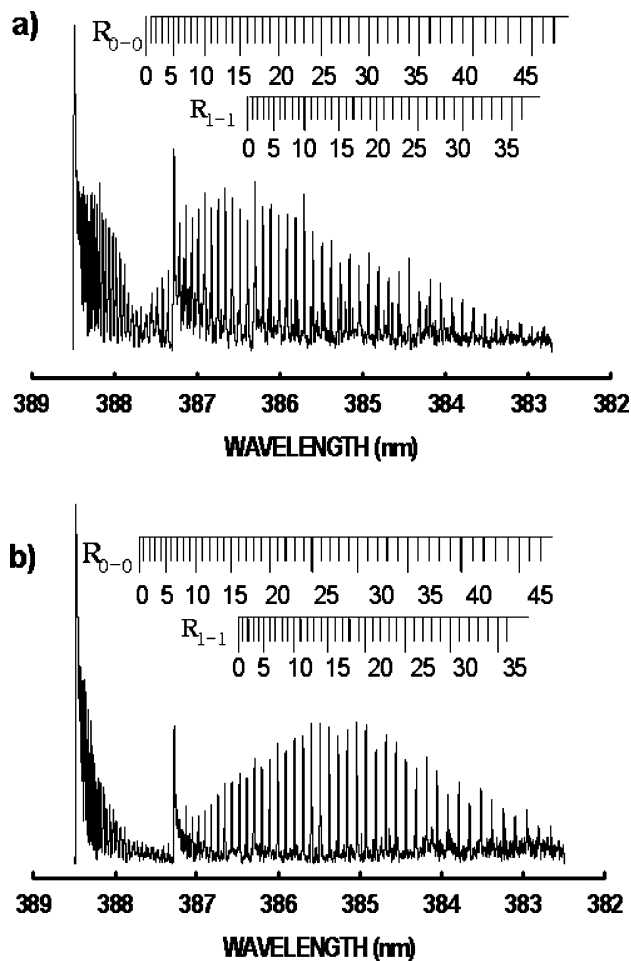


Figure 1. LIF spectra of CN produced from photodissociation of (a) cyclohexyl cyanide and (b) cyclohexyl isocyanide at 193 nm employing the B \leftarrow X electronic transition.

$N = 23 \pm 2$ for cyclohexyl cyanide and cyclohexyl isocyanide, respectively. The average rotational energies in CN from cyclohexyl cyanide and cyclohexyl isocyanide were thus obtained from the normalized distributions, which were 12.5 ± 1.3 kJ/mol and 21.1 ± 2.9 kJ/mol, respectively. Since the low-frequency bending modes of the CN group against the cyclohexyl group were excited by one or two quanta in room-temperature parent molecules (e.g., 113 and 153 cm⁻¹ for CN in-plane and out-of-plane wagging, respectively),¹⁴ these energies might be added to the observed rotational energies of the CN fragments. The vibrational population ratios in CN were also obtained from the integrated intensities of the P branch rotational transitions corrected by the Franck–Condon factors,¹⁵ which were 0.80/0.20 and 0.82/0.18 for $\nu = 0/1$ from cyclohexyl cyanide and cyclohexyl isocyanide, respectively.

B. Translational Energy Releases. To measure translational energies of the fragments, the Doppler profiles of the individual rotational transitions in the spectra were analyzed. The laser line profile was first measured from the rotational line profile after translational relaxation by collisions. A Doppler line profile of one of the low N rotational transitions was measured at a 2 μ s pump–probe delay and 5 Torr Ar, from which the laser line profile was measured after deconvolution of a Gaussian Doppler profile of CN at 300 K assuming complete relaxation. At this time delay and even higher pressures of Ar, no change in the profile and rotational relaxation to 300 K was observed. The estimated full width at half maximum of the Lorentzian laser line profile was 0.27 cm⁻¹.

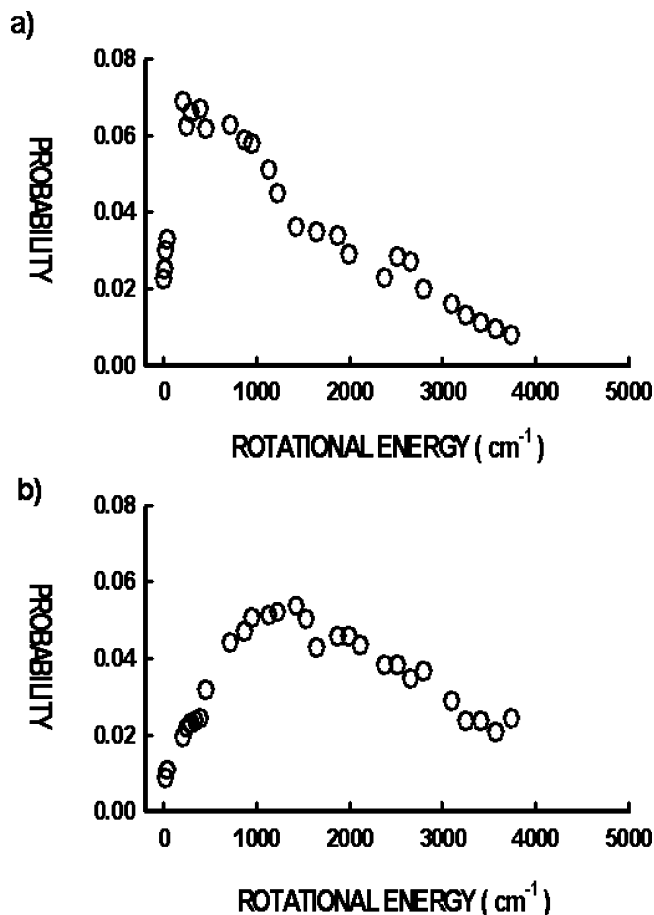


Figure 2. Rotational population distributions of CN measured from Figure 1 for (a) cyclohexyl cyanide and (b) cyclohexyl isocyanide.

In Figure 3, the Doppler-broadened spectra for $N = 14$ in the R branch rotational transitions from cyclohexyl cyanide and cyclohexyl isocyanide are presented. The rotational transitions from the two spin doublet states were nearly overlapped at low N and almost resolved at high N under the given resolution of our laser. Since the separation of the two transitions at $N = 14$ is 0.17 cm^{-1} , the measured profile was estimated as the sum of the two transitions with Gaussian profiles, assuming isotropic velocity distribution for CN. Then, the Gaussian Doppler profiles were extracted by deconvolution of the measured laser line profile. The average translational energy of CN at $\nu = 0$ and $N = 14$ was measured from the second moment of the profiles obtained from the best fit and then the center of mass translational energy releases in the products were calculated to be $83 \pm 15 \text{ kJ/mol}$ and $135 \pm 19 \text{ kJ/mol}$ for cyclohexyl cyanide and cyclohexyl isocyanide, respectively.

Discussion

A. Energy Partitioning. The dissociation energy of CN from cyclohexyl cyanide calculated from the heat of formation of cyclohexyl cyanide, cyclohexyl, and CN radicals obtained from literatures is $494.4 \pm 4.6 \text{ kJ/mol}$.¹⁶ Since no thermodynamic data for cyclohexyl isocyanide are available from the literature, the heat of formation of cyclohexyl isocyanide was calculated from ab initio calculations. For comparison, the dissociation energy of CN from cyclohexyl cyanide, which is 495.4 kJ/mol , was also obtained by the same ab initio calculations. The calculated dissociation energy of CN from cyclohexyl isocyanide is 409.2 kJ/mol , and the accuracy is expected to be similar to

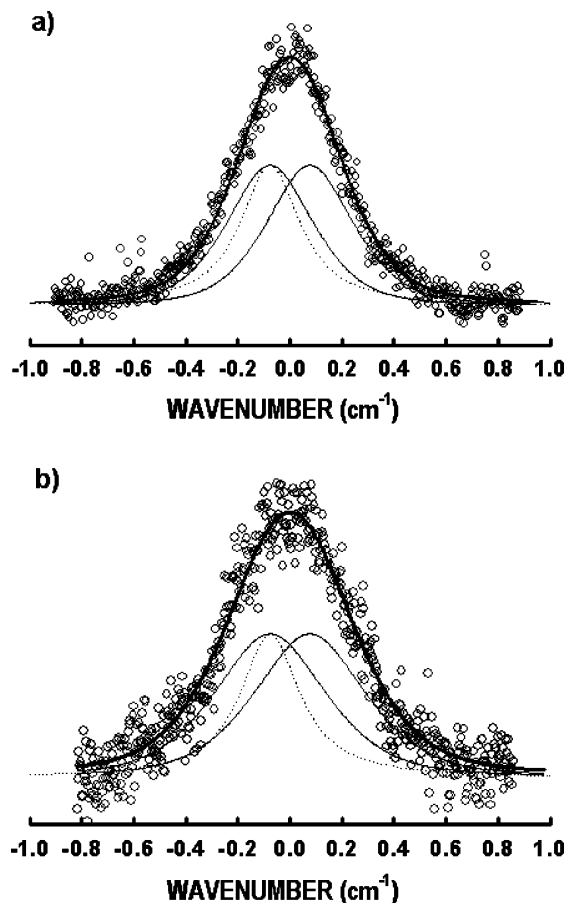


Figure 3. Doppler profiles of the R_{0-0} (14) rotational transitions of CN from photodissociation of (a) cyclohexyl cyanide and (b) cyclohexyl isocyanide. The solid lines are estimated Doppler profiles for individual rotational transitions, and the dotted lines are the measured laser line profiles (see text).

TABLE 1: Energies in the Products from Photodissociation of Cyclohexyl Cyanide and Cyclohexyl Isocyanide at 193 nm (kJ/mol)

E_{ave}^a	$\langle E_{\text{R}}(\text{CN}) \rangle$	$\langle E_{\text{T}} \rangle$	$E_{\text{int}}(\text{cyclohexyl})$
124.3	12.5 ± 1.3 (0.10) ^b	Cyclohexyl Cyanide	
		R(14)	83 ± 15 (0.67)
		R(43)	67 ± 13
210.5	21.1 ± 2.9 (0.10)	Cyclohexyl Isocyanide	
		R(14)	135 ± 19 (0.64)
		R(49)	81 ± 7

^a $E_{\text{ave}} = h\nu(193 \text{ nm}) - D_0 + \frac{3}{2}RT$ parent energy. ^b The quantity in parentheses is the fraction of the available energy.

that of cyclohexyl cyanide. Since the photon energy at 193 nm is 617.8 kJ/mol , including parent internal energies at room temperature, the available energies after dissociation are 124.3 and 210.5 kJ/mol for cyclohexyl cyanide and cyclohexyl isocyanide, respectively. In Table 1, the measured energy partitioning in the fragments are then listed as fractions of the available energies. The larger rotational energy of CN and larger translational energy release from the dissociation of cyclohexyl isocyanide than those of cyclohexyl cyanide may simply result from the larger available energy for the cyclohexyl isocyanide dissociation, but the fractions are remarkably similar, which would imply similar dissociation mechanisms for both molecules. It is also noted that the unusually large translational energy releases from the dissociation of such large molecules

would be the result of dissociation along strongly repulsive potential energy surfaces.

B. Electronic Transitions. The UV absorption spectra of cyclohexyl cyanide and cyclohexyl isocyanide both show continuously increasing absorption starting from around 210 nm. According to quantum chemical calculations, the HOMOs are π_{CN} for CH_3CN and a lone-pair orbital on C for CH_3NC , respectively.¹⁷ In both cases, the LUMO is π^* and the lowest-energy electronic transition excites the molecules to the π^* state where the equilibrium geometry is bent. In the spectra of CH_3CN , the first absorption band is assigned as the $\pi \rightarrow 3s$ Rydberg transition superimposed by the broad $\pi \rightarrow \pi^*$ transition with smaller transition probability. However, in CH_3NC , the first absorption band is assigned as the strongest $n \rightarrow \pi^*$ that is overlapped with the $n \rightarrow 3s$ Rydberg and the $\pi \rightarrow \pi^*$ transitions.² Assuming the similar absorption spectra for cyclohexyl cyanide and cyclohexyl isocyanide to CH_3CN and CH_3NC , an electronic transition at 193 nm would lead the molecules to the mixture of (π, π^*) and $(\pi, 3s)$ states for cyclohexyl cyanide and the mixture of mainly (n, π^*) and $(n, 3s)$ states for cyclohexyl isocyanide, respectively, from which the dissociation takes place. The measured energy distribution may reveal the contribution of each transition but unfortunately, the present experimental measurements cannot distinguish them in either case.

C. Dissociation Mechanism. To figure out the dissociation mechanism, consideration of spin correlation arguments is helpful. The dissociation products are cyclohexyl and CN radicals both in the spin-doublet ground electronic state. Although the threshold for producing CN in the A state from CH_3CN was reported as 188.4 nm,¹⁸ an attempt to detect CN by emission from the A state for the present study was failed, which ensures the CN radicals produced from cyclohexyl cyanide and cyclohexyl isocyanide at 193 nm are exclusively in the X state and there is not enough energy for producing electronically excited cyclohexyl radicals at this wavelength. Since each of the product radicals has two possible spin states, there are only four possible spin states that correlate to the pair of ground-state product radicals. One of them must be the ground singlet state, and the other three must be the three excited triplet states of the parent molecule, because the excited singlet state must correlate to either one of the product radicals being in the electronically excited state. Therefore, the dissociation at 193 nm must take place either from the ground state or the excited triplet states for both molecules.

In the case of ground-state dissociation, the dissociation occurs in the vibrationally hot ground electronic state following internal conversion from the initially excited state. In the hot ground state, fast intramolecular vibrational energy relaxation should take place, resulting in statistical energy partitioning among all degrees of freedom of the products. However, the measured average internal energy in CN is almost half of that in the much larger cyclohexyl radicals, which implies nonstatistical energy partitioning among products. Another argument that is against the ground-state dissociation is the dissociation rate. With 51 vibrational degrees of freedom in these molecules, the Rice–Ramsperger–Kassel–Marcus (RRKM) calculation with 497 kJ/mol bond energy and with only 124 kJ/mol excess energy shows that it should take over seconds or a minute for the necessary energy to be accumulated in one bond to be broken. During this time, the vibrationally hot molecules should be thermally deactivated by collisions with walls or other molecules producing no detectable CN for the present experimental time scale. In fact, it was reported that photodissociation of CH_3CN

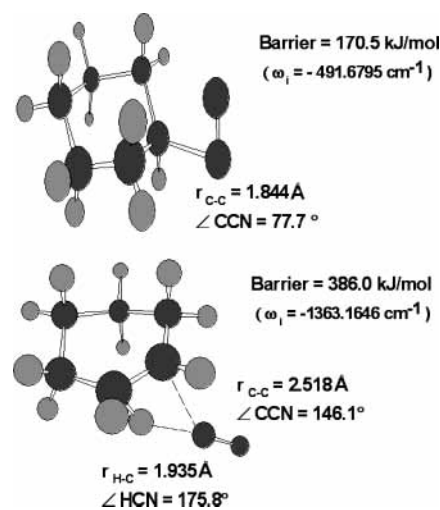


Figure 4. Optimized geometries of the transition states for isomerization between cyclohexyl isocyanide and cyclohexyl cyanide and molecular elimination reaction of HCN from cyclohexyl cyanide. The local maxima are identified from analyses of vibrational modes with one imaginary frequency.

and CH_3NC by VUV excitation produced CN from a long-lived intermediate state, and hence statistical energy partitioning was observed,² but the excess energy in this case is much higher and the molecules are much smaller. One might argue that, in the ground state, isomerization from cyclohexyl isocyanide to more stable cyclohexyl cyanide or molecular elimination of HCN or HNC should occur. Finding transition states and barriers for the isomerization and molecular elimination was attempted through similar ab initio calculations (Figure 4). With the calculated geometries and energies of the transition states, the RRKM rate was calculated to be $1.9 \times 10^9 \text{ s}^{-1}$ for the isomerization, but it still takes a long time for the dissociation of CN from cyclohexyl cyanide. Although the absolute quantum yields were not measured in the present experiments, all these possible pathways would be the cause of reducing the quantum yields for the CN production channel.

The electronic excitation at 193 nm in cyclohexyl cyanide and cyclohexyl isocyanide prepares these molecules in the excited singlet state, and the dissociation of CN takes place from the triplet states via curve crossing, which is strongly repulsive along the dissociation coordinates. The crossing rate should be fast judging from nonstatistical energy partitioning in the products, and the repulsive nature of the potential surfaces results in large translational energy releases experimentally measured for these molecules. The lifetime of molecules in the dissociative state could be measured from angular distribution of the products, which can be measured from translational anisotropies. But, unfortunately, the resolution of our probe laser was not high enough to resolve the Doppler profiles of the individual rotational transitions in the present study. One thing to be noticed is the distinct shape of the rotational population distribution of CN from cyclohexyl isocyanide, which is not Boltzmann-like (Figures 1 and 2). Similar rotational distributions were observed for CN in the photodissociation of ClCN and BrCN excited in the first UV absorption band.^{19,20} In this case, prompt dissociation occurs from the repulsive state and the distribution was explained by application of the rotational reflection principle, from which the shape of bending potential energy surfaces could be examined.²¹ Quantum mechanical reactive scattering calculations were also attempted for the H_2O_2 photodissociation, and the similar rotational distribution was predicted in the case of prompt dissociation from the repulsive surfaces.²² In the present

case of cyclohexyl isocyanide photodissociation, the observed non-Boltzmann rotational distribution may result from the dominant $n\pi^*$ character of the initially excited state, where the molecular geometry (C–N–C) is bent. However, further studies such as photodissociation as a function of excitation energies and/or theoretical studies on excited potential energy surfaces would be helpful to understand the dissociation dynamics in more detail.

Acknowledgment. This work was financially supported by the Korea Research Foundation.

References and Notes

- (1) Robison, P. J.; Holbrook, K. A. *Unimolecular Reactions*; Wiley: New York, 1972.
- (2) Ashfold, M. N. R.; Simons, J. P. *J. Chem. Soc., Faraday Trans. 2* **1978**, 174, 1263.
- (3) Moriyama, M.; Tsutsui, Y.; Honma, K. *J. Chem. Phys.* **1998**, 108, 6215.
- (4) Eng, R.; Filseth, S. V.; Carrington, T.; Dugan, H.; Sadowski, C. M. *Chem. Phys. Lett.* **1988**, 146, 96.
- (5) Blank, D. A.; Suits, A. G.; Lee, Y. T.; North, S. W.; Hall, G. E. *J. Chem. Phys.* **1998**, 108, 5784.
- (6) North, S. W.; Hall, G. E. *Chem. Phys. Lett.* **1996**, 263, 148.
- (7) Li, R.; Derecskei-Kovacs, A.; North, S. W. *Chem. Phys.* **2000**, 254, 309.
- (8) Oh, C. Y.; Shin, S. K.; Kim, H. L.; Park, C. R. *Chem. Phys. Lett.* **2001**, 342, 27.
- (9) Oh, C. Y.; Shin, S. K.; Kim, H. L.; Park, C. R. *J. Phys. Chem. A* **2003**, 107, 4333.
- (10) Park, J.; Yu, C.-F.; Bersohn, R. *Chem. Phys.* **1989**, 134, 421.
- (11) Frisch, M. J.; Trucks, G. W.; Schlegel, H. B.; Scuseria, G. E.; Robb, M. A.; Cheeseman, J. R.; Zakrzewski, V. G.; Montgomery, J. A.; Stratmann, R. E.; Burant, J. C.; Dapprich, S.; Millam, J. M.; Daniels, A. D.; Kudin, K. N.; Strain, M. C.; Farkas, O.; Tomasi, J.; Barone, V.; Cossi, M.; Cammi, R.; Mennucci, B.; Pomelli, C.; Adamo, C.; Clifford, S.; Ochterski, J.; Perderson, G. A.; Ayala, P. Y.; Cui, Q.; Morokuma, K.; Malick, D. K.; Rabuck, A. D.; Raghavachari, K.; Foresman, J. B.; Cioslowski, J.; Ortiz, J. V.; Stefanov, B. B.; Liu, G.; Liashenko, A.; Piskorz, P.; Komaromi, I.; Gomperts, R.; Martin, R. L.; Fox, D. J.; Keith, T.; Al-Laham, M. A.; Peng, C. Y.; Nagayakkara, A.; Gonzales, C.; Challacombe, M.; Gill, P. M. W.; Johnson, B. G.; Chen, W.; Wong, M. W.; Andres, J. L.; Head-Gordon, M.; Replogle, E. S.; Pople, J. A. *Gaussian 98*, Gaussian Inc.: Pittsburgh, PA 1998.
- (12) Engleman, R., Jr. *J. Mol. Spectrosc.* **1974**, 49, 206.
- (13) Earls, L. T. *Phys. Rev.* **1935**, 48, 423.
- (14) The vibrational frequencies were calculated by DFT calculations.
- (15) Nicholls, R. W. *J. Res. Natl. Bur. Stand.* **1964**, 684, 75.
- (16) (a) McMillen, D. F.; Golden, D. M. *Annu. Rev. Phys. Chem.* **1982**, 33, 493. (b) Berkowitz, J.; Ellison, G. B.; Gutman, D. *J. Phys. Chem.* **1994**, 98, 2744.
- (17) Ha, T.-K. *J. Mol. Struct.* **1972**, 11, 185.
- (18) Cody, R. J.; Dzvoni, M. J.; Glicker, S. *J. Chem. Phys.* **1985**, 82, 3100.
- (19) Halpern, J. B.; Jackson, W. M. *J. Phys. Chem.* **1982**, 86, 3528.
- (20) Lu, R.; McCrary, V.; Halpern, J. B.; Jackson, W. M. *J. Phys. Chem.* **1984**, 88, 3419.
- (21) Barts, S. A.; Halpern, J. B. *J. Phys. Chem.* **1989**, 93, 7346.
- (22) Zhang, D. H.; Zhang, J. Z. H. *J. Chem. Phys.* **1992**, 98, 6276.